# Casting Fe-Al-based intermetallics microalloyed with Li and Ag



| | |
|---|---|
| Journal: | *Journal of Materials Research* |
| Manuscript ID | Draft |
| Manuscript Type: | Metallic Materials Article |
| Date Submitted by the Author: | n/a |



| | |
|---|---|
| Complete List of Authors: | Villagomez-Galindo, Miguel; Universidad Michoacana de San Nicolas de Hidalgo, Facultad de Ingeniería Mecánica<br>Romo-Castaneda, Julio; Universidad Nacional Autonoma de Mexico, Facultad de Quimica<br>Bedolla-Jacuinde, Arnoldo; Universidad Michoacana de San Nicolas de Hidalgo, Instituto de Investigación en Metalurgia y Materiales<br>Carbajal-De la Torre, Georgina; Universidad Michoacana de San Nicolas de Hidalgo, Facultad de Ingeniería Mecánica<br>González-Rojas, Hernan; Universitat Politecnica de Catalunya, Departament of Mechanical Engineering<br>Espinosa-Medina, Marco; Universidad Michoacana de San Nicolas de Hidalgo, Facultad de Ingeniería Mecánica |



| | |
|---|---|
| Key Words: | casting, alloy, microstructure |


SCHOLARONE™
Manuscripts

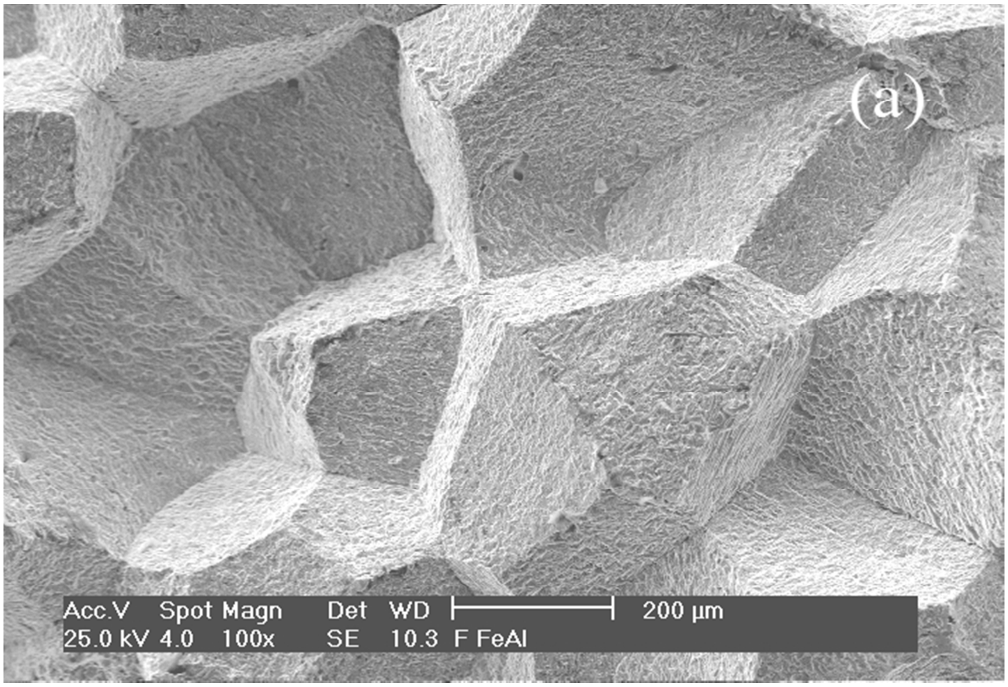


Figure 6. SEM images at x100 magnification of specimens fractured by the tension test of: a) Alloy-A,
241x180mm (75 x 68 DPI)

Review

# Casting Fe-Al-based intermetallics microalloyed with Li and Ag

M. Villagomez-Galindo[1,4], J.C. Romo-Castañeda[2], A. Bedolla-Jacuinde[3] G. Carbajal-De la Torre[1], H.A. González-Rojas[4], M.A. Espinosa-Medina [1,]*

[1] Facultad de Ingeniería Mecánica, UMSNH. 58000, Morelia, México.

[2] Facultad de Química, UNAM. 04510 México, D.F., México

[3] Instituto de Investigación en Metalurgia y Materiales, UMSNH. 58000, Morelia, México.

[4] Departament of Mechanical Engineering (EUETIB), Universitat Politécnica de Catalunya, Spain

Corresponding author: * marespmed@gmail.com; Tel. +52 4431646635

For Peer Review

**ABSTRACT**

The effect on the mechanical properties at room temperature of Li and Ag additions to the Fe-Al (40 at.%)-based alloy produced by conventional casting were evaluated in this work. Microalloying elements were added into a previously molted Fe-(40 at.%) aluminium-based alloy, stirred, and then cast into sand moulds to directly produce tensile specimens. In order to determine the mechanical properties, tensile tests and hardness measurements were performed. The additions of both Ag and Li showed an increase in ductility and tensile strength of the intermetallic alloys. In addition, micro-hardness was substantially increased with the Li addition. Lithium additions promoted a solid solution hardening, whereas Ag additions promoted ductility due to a microstructural modification and to the formation of a soft $Ag_3Al$ phase. Characterization by both optical and electronic microscopy, EDS microanalysis, and X-ray diffraction supported the mechanical characterization.

**Keywords:** **A** Iron aluminides; B Microalloying; F Mechanical properties at room temperature; F Fracture mode.

## 1. INTRODUCTION

In the past, the Fe-Al-based intermetallic alloys had been studied with interest due to their excellent corrosion resistance and their potential application in the energy conversion industries as structured materials [1-7]. However, the use of those alloys as structural components had been limited due to their brittle fracture behavior and low ductility properties at room temperatures resulting from environmental embrittlement, weak grain boundaries, vacancy hardening, and embrittlement [7]. Environmental embrittlement involves moisture in air, which is the major cause of low tensile ductility. Such environmental embrittlement is the consequence of a chemical reaction involving the reaction of Al with oxygen from moisture, releasing hydrogen atoms that could be adsorbed [8]. However, there are other factors that can modify mechanical behavior at room temperature, such as grain size, improving ductility as the grain size is reduced [9]. The quantity of Al in the FeAl alloy systems also has an important effect on both the mechanical properties [10] and corrosion resistance at high temperature applications [7]. By reason of this, a best condition for those properties for high temperature applications has been reported for Al concentrations between 35 and 45 at.% [7,10-12]. This has become the baseline for the production of those alloys.

Hence, the production of alloys by the abovementioned conventional methods is of industrial interest due to its low cost. In this sense, the induction melting and casting processing is one of

For Peer Review

the procedures that is also used for producing these FeAl alloys [7,10-13] and it could be sequenced by work-hardening [10,12] and/or heat treatment [11,13] processes in order to change the mechanical properties of the base alloy. In addition, microalloying with ternary elements is also useful for improving mechanical properties and hot corrosion resistance. The microalloying process during melting is a very easy way to incorporate a third alloying element, which can be done as a solid solution [14] or segregated phases. The effect of alloying Fe-Al by third elements on the mechanical properties at room temperature has been studied before [4,5,13-21] with different results. Furthermore, the alloying effects on those mechanical properties of both the grain refinement and the environmental interaction have been evaluated [15,16,20-23].

In this way, the alloying effect on the mechanical properties at room temperature of materials produced by the induction melting process becomes very interesting. Hamana et al. [13] reported that the increase of Cr additions to a Fe-28 at.% Al stabilized the B2 phase of the microstructure, which, in turn, increased its microhardness when a heat treatment was applied, due to the modification of the B2 to $D0_3$ transition rate. Similarly, grain size modification [17], third phase formations, and carbide precipitation [16,18] are important factors for improving mechanical properties. Salazar et al. [19] observed a notable increase in ductility under compression tests at room temperature when Li was added to an FeAl intermetallic. Rosas et al [15] have also reported an increase in ductility when adding Li to an $Fe_3Al$-based alloy, but under tensile loads. However, the effect on the mechanical properties by adding Ag to an FeAl-based alloy has not been reported. As a first step for a future high temperature assessment, the effects on the mechanical properties at room temperature of Li and Ag additions to an Fe-40 at.% Al-based alloy, produced by conventional casting, were evaluated in this work. The alloys were

For Peer Review

metallographic and chemically characterized by light microscopy, scanning electronic microscopy (SEM), X-ray diffraction, and energy dispersive spectroscopy (EDS).

## 2. EXPERIMENTAL PROCEDURE

The experimental alloys were produced in an induction furnace by using a silicon carbide crucible [24]. In order to produce Fe-40 at.%Al-based intermetallic alloys with additions of 1 and 3 at.% of Li and Ag, high purity raw materials were used (99.9% of purity). Table 1 summarizes the designed atomic chemical composition of the intermetallic cast alloys. An Inductotherm induction furnace using an argon protection atmosphere was employed to cover the liquid iron and aluminum was then added and mechanically stirred. Finally, the microalloying element was added, followed by a stirring for full dissolution and homogenization. To avoid losses by evaporation, the addition of Li was realized using an aluminum capsule in order to minimizing the spontaneous reaction of Li in the casting. The melt was cast into sand moulds to produce next-to-shape tensile specimens directly from casting. Mechanical properties were measured by tensile tests according to the ASTM E8 standard [25]. They were carried out on a Shimadzu (UH-300kNI) universal testing machine at a strain rate of 0.4 mm/min. Hardness was measured in a Shimadzu (HMV-2) hardness tester by applying 100 g of load for 20 s with a diamond indenter [26]. Prior to the mechanical characterization, intermetallic alloys were isothermally heat-treated at 800 °C for 48 hours in order to reduce the adsorbed hydrogen contents.

Samples with a size close to 10 mm x 10 mm x 5 mm were cut from the castings, grinded, polished up to 0.5 μm, and then etched for metallographic characterization. Chemical etching was performed using Keller's etchant (HCl, $HNO_3$, HF, and $H_2O$) [27]. Stoichiometric

For Peer Review

characterization of the phases present in each alloy was determined by x-ray diffraction patterns, using Cu-kα radiation in a two-theta range from 20 to 100° in a SIEMENS 5000 diffractometer. Optical microscope observation was done using a Nikon Epiphot 300 equipped with a digital camera for imaging. Scanning electron microscopy was performed for imaging characterization and microanalysis by energy dispersive spectroscopy (EDS) in a Phillips ESEM-XL30 equipped with an EDAX.

For Peer Review

## 3. RESULTS AND DISCUSSION

### *3.1. Microstructural and chemical characterization*

The macrostructure of the as-cast Fe-(40%at.Al)-based alloys was modified with the addition of a third alloying element. Figure 1 shows the optical image of metallographies at low magnifications of the base alloy and FeAl with 3 %at.Li and 3 %at.Ag (Alloy-A, Alloy-C, and Alloy-E). The base FeAl intermetallic showed a columnar grain distribution from the periphery towards the center bar in the opposite direction of the heat flow (Fig.1a). This characteristic morphology was identified (and described further ahead) with a low amount of the $Fe_3Al$ phase homogeneously distributed into the FeAl matrix. The addition of Li to the base alloy improved a change in the appearance of the solidified macrostructure. The main observation was the modification of macro-grains: they changed from a columnar to an equiaxial shape; it is suggested that they form due to a higher nucleation process during solidification. Thus, it was to be expected when equiaxed grains formed at the end of the solidification (in the center of the bar) and the percentage of this solidification mode was proportional to the quantities of Li addition

(Fig.1b). A similar behavior was shown by the alloys with Ag addition (1, 3 at. %) (Fig.1c). However, those alloys showed a third phase formation, a singular phase containing high amounts of Ag and Al, almost at 3:1 ratio. This third phase increased with the addition of Ag (Fig.1c).

Figure 2 shows the detailed microstructure of all alloys observed by SEM at higher magnifications. Figure 2a displays the morphologies of the structural phases of the base FeAl. The base alloy was composed of two phases: the small amount of the $Fe_3Al$ phase homogeneously dispersed into the major phase of FeAl, as described above, and in agreement with the X-Ray diffraction results and EDS (Fig 2b) [24]. The minor phase showed size variations, up to 20 μm in length and an average width of 3 to 7 μm. The minor phase solidified as a dendritic mode with primary and secondary arms of around 5 μm in diameter. Li additions promoted the modification of such a type of morphology and decreased the amount of the $Fe_3Al$ minor phase (Fig.2c and Fig.2d). It was suggested that this decrease was caused by an incorporation of solid solution, according to the X-ray diffraction results [24]. On the other hand, Ag additions promoted the formation of a third phase, identified as an $Ag_3Al$ intermetallic compound. Similarly to the Li additions, the Ag alloying promoted the modification of the microstructural morphology by decreasing the amount of $Fe_3Al$ (Fig.2e, Fig.2f) and, in turn, increasing the amount of $Ag_3Al$.

The EDS analysis carried out for all the observed phases showed the semi-quantitative stoichiometry of the compounds. Those analyses corresponded to the atomic ratio of the FeAl, $Fe_3Al$, and $Ag_3Al$ intermetallic compounds verified by x-ray diffraction (described further ahead). The SEM characterization showed that the second phases in the base FeAl alloy presented a

For Peer Review

quasi-regular distribution (Fig.2a). Additions of Li led to a refinement of the minor phase, showing a uniformly distributed needle shape (Fig.2c). X-ray diffraction results did not present patters of Li or Li compounds; we suggest Li remains in solid solution into the base alloy. Also, close to 0.5 at.% of Ag was incorporated in solid solution in the FeAl+Ag(1,3 at.%) alloys. In those alloys, the excess of Ag concentration segregated towards the solidification front, as $Ag_3Al$ (Fig.2e, Fig.2f). Similarly, the $Fe_3Al$ phase was refined and showed a needle shape, as did the FeAl+ Li alloy. The effect of the third alloying element (Li and Ag) on the refinement of the $Fe_3Al$ phase could be due to the ability of iron to occupy sublattice sites, originally occupied by aluminum, through an excess of iron atoms. This is known as the antisite defect [6]. It is suggested that microalloying may promote a decrease in the occupied sites by Fe in the FeAl B2 lattice, hence decreasing the Fe contents for $Fe_3Al$ formation, which, in turn, decreases the amount of this later phase.

For Peer Review

Figure 3 shows the x-ray diffraction patterns obtained for the FeAl-based alloys according to PCPDF based data patterns: 28-0034 ($Ag_3Al$), 65-6132 (FeAl) and 65-5188 ($Fe_3Al$). Alloy-A showed the FeAl and $Fe_3Al$ phases; see the microstructure of Alloy-A (Fig.2a). Similarly, Alloy-B and Alloy-C showed those phases with no other phase formation when Li was added, since it suggested this element entered into the solid solution, and its effect was only reflected on the microstructure and mechanical properties, as will be discussed later. On the other hand, Ag additions to the base FeAl (Alloy-D and Alloy-E) did indeed promote a third phase formation during the solidification process, identified as $Ag_3Al$ (Fig.3). Figure 4, shows the EDS spectra of the FeAl+Ag matrix and the segregated particles of the Ag rich phase. The matrix showed limited Ag solubility, between a 0.4 to 0.6 Ag at.% content (fig.4a), whereas the segregated phase showed a much higher amount of Ag. The Ag additions had two types of interaction with the base FeAl alloy. An amount of approximately 0.5 at.% Ag atoms entered into the B2 crystalline lattice through the substitutional solid solution (Fig.4a), and the remaining amount of Ag was segregated towards the solidification front, forming the $Ag_3Al$ phase (Fig.4b). A similar effect has been observed with Mo addition to a FeAl due to the $Mo_3Al$ phase formation [4].

### *3.2. Mechanical characterization*

The addition of both Ag and Li to the FeAl-based alloy promoted some changes in the mechanical properties. Both elements increased the ductility and tensile strength of the base alloy, as well as the microhardness. A previous report on the mechanical evaluation of an FeAl (36.5% Al) alloy showed brittle cleavage fracture and only 2.2% tensile elongation when tested in air at room temperature, but the same alloy tested in a conventional vacuum had a ductility of about 8% [7]. The addition of Li to the base FeAl improved the solid solution hardening effect, which is suggested to be due to the small size of this atom that promotes a similar effect as carbon or Mo [4,28]. Our work shows no evidence of the precipitation of hard Fe-Al-carbides and $Mo_3Al$, as reported elsewhere [4,28]. Tensile and microhardness results of the FeAl-based alloy are shown in Figure 5 and summarized in Table 2. Yield strength of a brittle material was calculated with the ultimate tensile strength (UTS), as recommended by the ASTM E8 standard [25].

The FeAl-based alloy presented a UTS value of 390 MPa in air at room temperature (Table 1). Morris et al [10] have reported that yield stress increases with Al content up to 25%, and it decreases rapidly in the 25-28% Al range, but shows little increase over the 30-40% Al range. They described ductility as an inverse relationship to the yield stress, with a rapid fall in ductility

For Peer Review

up to 25% Al, a slight maximum at 28% Al, and a steady, slow fall thereafter. The yield stress and ductility of the base FeAl in the present work is in agreement with the observations of Morris et al. [10]. Furthermore, Kupta [11] reports a 360 MPa strength value at room temperature, but it was tested in an argon atmosphere for the B2 structured Fe-45Al-4Cr-0.1Zr-0.02B alloy and this alloy was melted in a vacuum induction furnace, with casting and homogenizing at 1000 °C/72 h. In our work, the additions of Li to the FeAl-based alloy improved the mechanical properties, showing UTS values of 448 and 568 MPa (Fig.5) and elongation increasing between 25 % and 30 % for Alloy-B and Alloy-C, respectively. Similar increases of UTS values of FeAl alloys have been obtained with additions of carbon [28] or molybdenum [4]. Salazar et al. [19] reported similar effects when adding Li to a similar alloy, but tested under compressive stress. The effects of Ag additions were more meaningful in the elongation results, increasing from 20% to 50% for 1 and 3 (at.%) of Ag, respectively. However, a small increase in UTS values was observed, around 366 and 433 MPa (Fig.5; alloy-4 and Alloy-5). Ductility of the FeAl-based alloy was increased with Ag % addition.

### *3.3. Fractographic characterization*

The results of mechanical strength and hardness showed a direct correlation with Li addition contents, but this was not seen in relation to elongation, which was similar at the 1 and 3 % Li content. On the other hand, Ag additions did not significantly improve strength. However, elongation was higher than in the alloys with Li additions, particularly the alloy with 3 at.% of Ag. Ductility in the FeAl+Ag systems was increased in proportion to the Ag addition. This effect is explained in terms of the third phase formed in the alloys, which allowed the plastic displacement among the grain faces of both the FeAl and $Ag_3Al$ phases (Fig.2). In this sense,

For Peer Review

fracture morphology of the tensile tests provided more evidence of the plasticity or hardening effect of the Li and Ag additions. Figure 6 shows the SEM images of the resulting fractographs of the tensile tests of the FeAl-based alloys.

The effect of the third element addition on the increase of elongation was more evident when Ag rather than Li was added. Namely, the maximum elongation % at strain condition was increased by Alloy-E (around 50% vs base FeAl, table 2), whereas (1, 3 at.%) Li addition promoted an increasing change of around 30 %. However, characteristic brittle fractures were observed on all alloys (Fig.6). Alloy-A showed intergranular failure mode by grain decohesion (Fig.6a), associated with $\langle 111 \rangle$ or $\langle 100 \rangle$ slips [6], but it was modified by the third alloying additions, particularly with the Ag additions. Due to the plasticity improvement of the Ag additions, the fracture mode was changed from only intergranular to a mixture of intergranular and transgranular fracture (Fig.6d and Fig.6e). On a minor level, Li additions promoted a fraction of transgranular fracture mode mixed with intergranular decohesion of the strongly anchored columnar grains, as an effect of the increase in strength (Fig.6b and Fig.6c). This long intergranular failure mode occurred parallel to the columnar grain length.

FeAl intermetallic alloys did not show an apparent yield point discontinuity on the tensile tests, (Fig.5). This behavior is typical of brittle alloys. However, some level of ductility was evidenced by the increase in the percent of elongation at strain condition with the Ag addition (Fig.6) and the characteristic fracture mode. The change in the fracture mode for these alloys showed a transition from intergranular to transgranular and cleavage fracture, as previously reported [21]. That fracture mode was caused by the addition of ternary elements, and in this way the effect of

For Peer Review

Li represented an increase of around 44 % in the ultimate tensile strength (UTS). Although tensile tests were not carried out in a controlled environmental atmosphere, the results could be comparable to those obtained when studying the effect of the environment and the strain rate on tensile properties of FeAl crystals by Wu and Baker [23]. In addition, those results also concur with the results obtained by Pike and Liu [20], who studied the effect of vacancies on the environmental yield strength dependence of boron-free and boron-doped Fe-40Al. They reported an increase of almost 200 MPa of UTS on tests carried out in a vacuum, compared with the same alloys tested in air. The UTS values of the vacuum tests are similar to the UTS value shown by the Alloy-C in the present work. A lower effect on UTS behavior was shown by the other Ag addition alloys (Alloy-D and E) and the increase in the percentage of transgranular fracture, which evidences cleavage facets promoted by the presence of the $Ag_3Al$ ductile phase, has also been previously observed [21].

For Peer Review

The change in the ductility of the base FeAl alloy represented by an increase in the elongation percentage is attributed to the modification of the microstructures. Similar results were reported by Huang [16] and Chao et al. [22]. The former studied the influence of microstructure and test conditions on the tensile behavior of FeAl-based alloys with Mo, Nb, Zr, and C, which effectively increased the strength properties [16]. The latter analyzed that influence with $Y_2O_3$ particles (18 and 150 nm) and found that the major changes of strength were obtained by the grain refinement. They reported an increase of ductility of about 10% associated with grain size ranging from 1 to 100 μm [22]. Of course, the environmental control and surface finishing of the samples were very closely controlled. In the present work, the strengthening modification was attributed to the microstructure refinement in the base FeAl by the Li addition through redistribution and shape modification of the $Fe_3Al$ phase (Fig.2). The increase in hardness was associated with the microstructural modifications by means of the combined contributions of vacancy hardening into an ordered and disordered domain/particle between grain borders and phases generated by the Li addition [29]. On the other hand, the softening effects due to the Ag additions were associated with the decreased $Fe_3Al$ phase and the formation of the third $Ag_3Al$ phase. In that case, the ordered and disordered vacancy hardening was not associated with the decrease of hardening, but was related to the third soft phase, which enhanced the plastic behavior. These results are in agreement with those reported by Cielsar et al [18], who studied the influence of Cr and Ce additions on the mechanical properties of the Fe-(28 at.%)Al system, which promoted the precipitation of Cr–Fe–(C) particles, decreasing the hardness of the alloy with a Cr content. In summary, the additions of Li and Ag to the Fe-(40 at.%)Al-based alloys increased the tensile strength at room temperature, due to the contribution of both the solid solution hardening and the vacancy increasing in the microstructures. Additionally, the increase of ductile behavior was promoted by the microstructural changes, which had an important effect on slip plains, but the main contribution was attributed to the formation of the soft $Ag_3Al$ phase in the Ag content alloys.

## 4. CONCLUSIONS

The additions of both Ag and Li into the FeAl-based alloy led to increased ductility and tensile strength. Li promoted a direct increase on strength and hardness due to solid solution hardening effects, but it caused no significant changes in ductility. On the other hand, Ag additions did not significantly improve the strength properties. However, this addition promoted an elongation higher than that of the alloys with Li additions, particularly for the 3 at.% of Ag alloy. Ductility was observed to increase with the Ag content.

For Peer Review

Changes in the fracture mode were also observed when alloying the FeAl. The change in the fracture mode for these alloys showed a transition from intergranular to transgranular and cleavage fracture. Li additions caused an approximately 50% increase in the UTS, whereas a lower effect was shown by the Ag addition. Additionally, Ag additions could increase the percentage of transgranular fracture due to the presence of the ductile phase.

Additions of Li and Ag to the Fe-(40 at.%)Al based alloys increased the tensile strength at room temperature due to the contribution of both the solid solution hardening and the vacancy increasing in the microstructures. Additionally, the increase in ductility was promoted by the microstructural change, which had an important effect on slip planes, but the primary contribution was attributed to the formation of the soft $Ag_3Al$ phase in the $Fe_{60}Al_{40}$-(1,3)Ag alloys.

For Peer Review

**Acknowledgements**

The present research was supported by CONACYT for the project financing Number: 243236, CB-2014-02, I0017 Fund.

**References**

1. F. Charlot, E. Gaffet, B. Zeghmati, F. Bernard, J.C. Niepce, Mechanically activated synthesis studied by X-ray diffraction in the Fe-Al system, Mat Sci Eng A262 (1999) 279-288.
2. M. Kupka, Technological plasticity studies of the FeAl intermetallic phase-based alloy, Intermetallics 12 (2004) 295-302.
3. W. J. Zhang, R. S. Sundar, S.C. Deevi, Improvement of the creep resistance of FeAl-based alloys, Intermetallics 12 (2004) 893-897.

4. M. Eumann, M. Palm, G. Sauthoff, Alloys based on $Fe_3Al$ or FeAl with strengthening $Mo_3Al$ precipitates, Intermetallics 12 (2004) 625-633.
5. A. O. Mekhrabov, M. V. Akdeniz, Effect of ternary alloying elements addition on atomic ordering characteristics of Fe-Al intermetallics, Acta Mater 47 (1999) 2067-2075.
6. I. Baker, P.R. Munroe, Mechanical properties of FeAl, Int Mater Rev 42 (1997) 181-205.
7. C.T. Liu, E.P. George, P.J. Maziasz, J.H. Schneibel, Recent advances in B2 iron aluminide alloys: deformation, fracture and alloy design, Mat Sci Eng A258 (1998) 84-98.
8. N.S. Stoloff, C.T. Liu, Environmental embrittlement of iron aluminides, Intermetallics 2 (1994) 75-87.
9. I. Baker, O. Klein, C. Nelson, E.P. George, Effects of boron and grain-size on the strain-rate sensitivity of Fe-45Al, Scripta Metall Mater 30 (1994) 863-868.
10. D.G. Morris, M.A. Munoz-Morris, L.M. Requejo, Work hardening in Fe–Al alloys, Mat Sci Eng A460–461 (2007) 163-173.
11. M. Kupka, Temperature dependence of the yield stress of an FeAl base alloy, Mat Sci Eng A336 (2002) 320-322.
12. L. Pang, K. S. Kumar, Mechanical behavior of an Fe-40Al-0.6C alloy, Acta Mater 46 (1998) 4017-4028.
13. D. Hamana, L. Amiour, M. Bouchear, Effect of chromium ternary additions on the ordering behaviour in Fe–28 at.% Al alloy, Mater Chem and Phys 112 (2008) 816–822.
14. J.H. Schneibel, Strengthening of iron aluminides by vacancies and/or nickel, Mat Sci Eng A258 (1998) 181-186.
15. G. Rosas, R. Esparza, A. Bedolla-Jacuinde, R. Perez, Room temperature mechanical properties of $Fe_3Al$ intermetallic alloys with Li and Ni additions, J Mater Eng Perform 9 (2009) 57-65.


For Peer Review

16. Y.D. Huang, L. Froyen, On the effect of microstructural parameters on tensile properties of a high work-hardening $Fe_3Al$-based alloy, Intermetallics 11 (2003) 361-372.

17. A. Wasilkowska, M. Bartsch, F. Stein, M. Palm, G. Sauthoff, U. Messerschmidt, Plastic deformation of Fe-Al polycrystals strengthened with Zr-containing laves phases - Part II. Mechanical properties, Mat Sci Eng A381 (2004) 1-15.

18. M. Cieslar, M. Karlık, M. Benko, T. Cernoch, The influence of Cr and Ce additions on the mechanical properties of $Fe_3Al$ based alloys, Mat Sci Eng A324 (2002) 23-27.

19. M. Salazar, A. Albiter, G. Rosas, R. Perez, Structural and mechanical properties of the AlFe intermetallic alloy with Li, Ce and Ni additions, Mat Sci Eng A351 (2003) 154-159.

20. L.M. Pike, C.T. Liu, The effect of vacancies on the environmental yield strength dependence of boron-free and boron-doped Fe-40Al, Intermetallics, (2000) 1413-1416.

21. P. Hausild, M. Karlik, J. Siegl, I. Nedbal, Fractographic analysis of the crack growth in the Fe3Al based intermetallic alloy, Intermetallics 13 (2005) 217-225.

22. J. Chao, D.G. Morris, M.A. Muñoz-Morris, J.L. Gonzalez-Carrasco, The influence of some microstructural and test parameters on the tensile behaviour and the ductility of a mechanically-alloyed Fe-40Al alloy, Intermetallics 9 (2001) 299-308.

23. D. Wu, I. Baker, The effect of environment and strain rate on the room temperature tensile properties of FeAl single crystals, Intermetallics 9 (2001) 57-65.

24. J. C. Romo Castañeda, "Caracterización de una Aleación Fe-Al", Tesis de Licenciatura, (2006), Facultad de Química, UNAM.

25. ASTM Designation: E 8M, "Standard Test Methods for Tension Testing of Metallic Materials [Metric]" (2001) 1-22.

26. ASTM Designation: E3, "Standard Guide for Preparation of Metallographic Specimens" (2001) 2-13.

For Peer Review

27. ASTM Designation: E 407, "Standard Practice for Microetching Metals and Alloys" (1999) 1-21.

28. R.G. Baligidad, A. Radhakrishna, Effect of carbon and processing on structure and mechanical properties of Fe-11 wt.% Al alloy, Mat Sci Eng A283 (2000) 211–217.

29. X. Amils, J. Nogues, S. Suriñach, M.D. Baro, M.A. Muñoz-Morris, D.G. Morris, Hardening and softening of FeAl during milling and annealing, Intermetallics 8 (2000) 805-813.

For Peer Review

**Tables and figure captions**

Table 1. Chemical composition of intermetallic alloys

Table 2. Strength-strain parameters (***σ, ε***) and hardness measurements of FeAl-based alloys

Figure 1. Metallographic images observed by light microscopy of a) Alloy-A, b) Alloy-C, and c) Alloy-E.

Figure 2. SEM micrographs observed for a) Alloy-A, b) EDS chemical analysis of Alloy-A, c) Alloy-B, d) Alloy-C, e) Alloy-D, and f) Alloy-E.

Figure 3. X-ray spectrums obtained on the FeAl-based and FeAl+(Li, Ag) intermetallic alloys (summarized in table 1).

Figure 4. EDS chemical analysis of FeAl with Ag additions a) matrix phase and b) Ag rich segregated phase (segregated from Alloy-D).

Figure 5. Strength-strain plots of tensile test from FeAl-based alloys.

Figure 6. SEM images at x100 magnification of specimens fractured by the tension test of: a) Alloy-A, b) Alloy-B, c) Alloy- Alloy-C, d) Alloy-D, and e) Alloy-E.

For Peer Review

**Table 1**

| $Fe_{60}Al_{40}$-based Alloy | + at.% Li | + at.% Ag |
|---|---|---|
| Alloy-A | - | - |
| Alloy-B | 1 | - |
| Alloy-C | 3 | - |
| Alloy-D | - | 1 |
| Alloy-E | - | 3 |

**Table 2**

| Alloy | Hardness (Hv), MPa | *E* module MPa | UTS, MPa |
|---|---|---|---|
| Alloy-A | 379.8 | 16703 | 390 |
| Alloy-B | 432.6 | 15531 | 448 |
| Alloy-C | 476.0 | 21773 | 568 |
| Alloy-D | 323.8 | 13793 | 366 |
| Alloy-E | 363.8 | 11569 | 433 |

For Peer Review

**Fig.1**

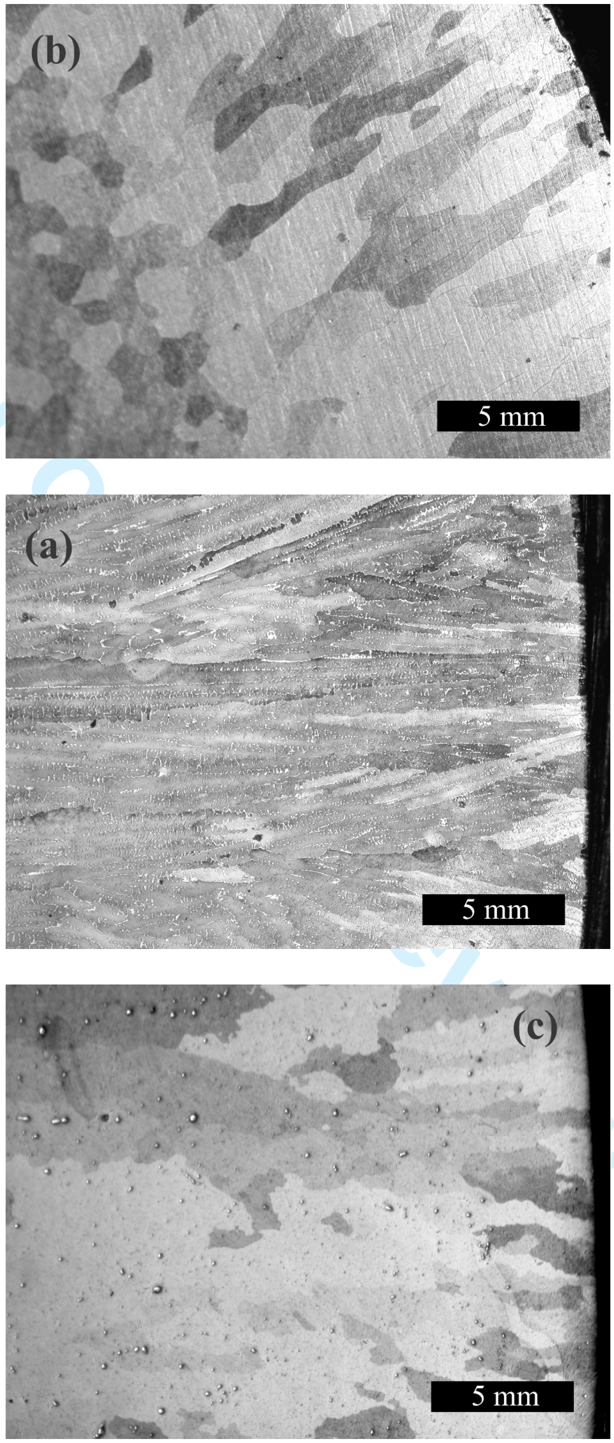

**Fig.2**

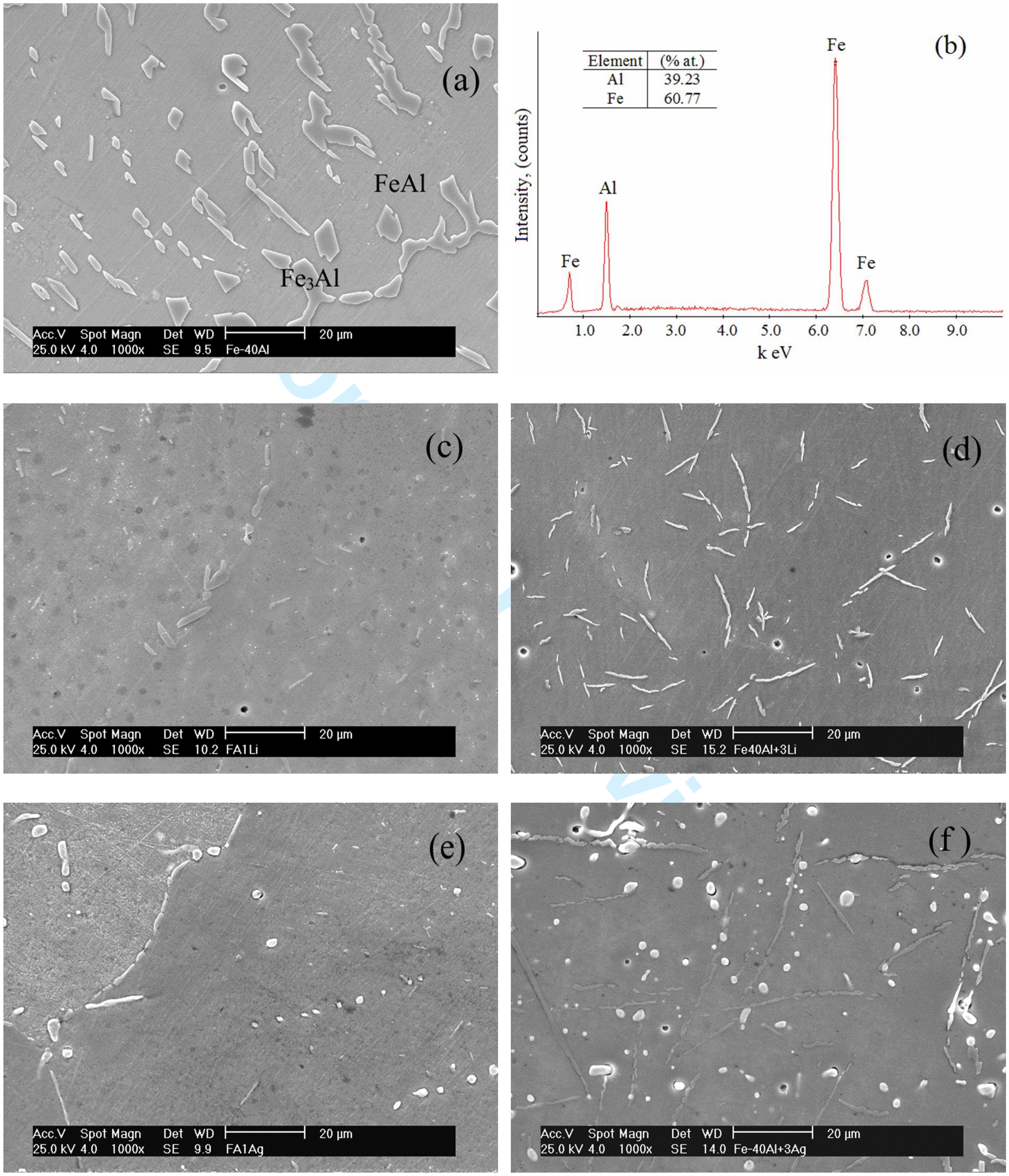
(a)
FeAl
Fe3Al
Acc.V Spot Magn Det WD 20 µm
25.0 kV 4.0 1000x SE 9.5 Fe-40Al
(b)
Element (% at.)
Al 39.23
Fe 60.77
Intensity, (counts)
Fe
Al
Fe
Fe
1.0 2.0 3.0 4.0 5.0 6.0 7.0 8.0 9.0
k eV
(c)
Acc.V Spot Magn Det WD 20 µm
25.0 kV 4.0 1000x SE 10.2 FA1Li
(d)
Acc.V Spot Magn Det WD 20 µm
25.0 kV 4.0 1000x SE 15.2 Fe40Al+3Li
(e)
Acc.V Spot Magn Det WD 20 µm
25.0 kV 4.0 1000x SE 9.9 FA1Ag
(f )
Acc.V Spot Magn Det WD 20 µm
25.0 kV 4.0 1000x SE 14.0 Fe-40Al+3Ag

Fig.3

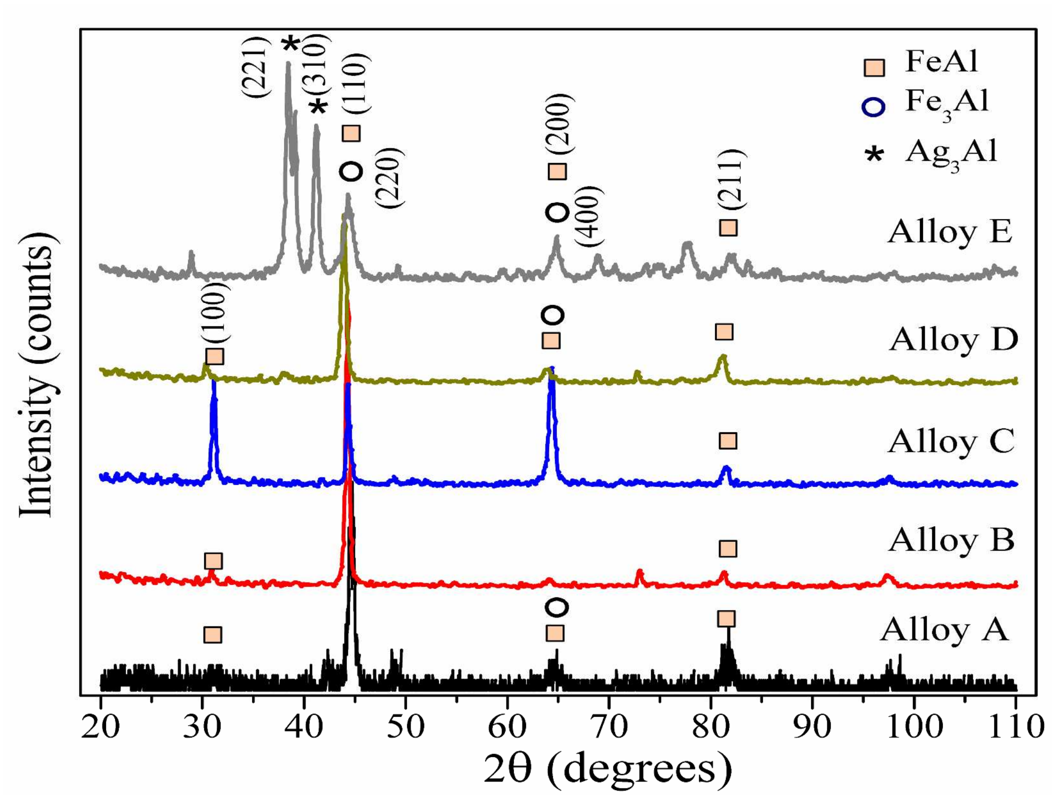
FeAl
Fe$_3$Al
Ag$_3$Al
(221)
(310)
(110)
(220)
(200)
(400)
(211)
(100)
Alloy E
Alloy D
Alloy C
Alloy B
Alloy A
Intensity (counts)
20 30 40 50 60 70 80 90 100 110
2θ (degrees)

Fig.4

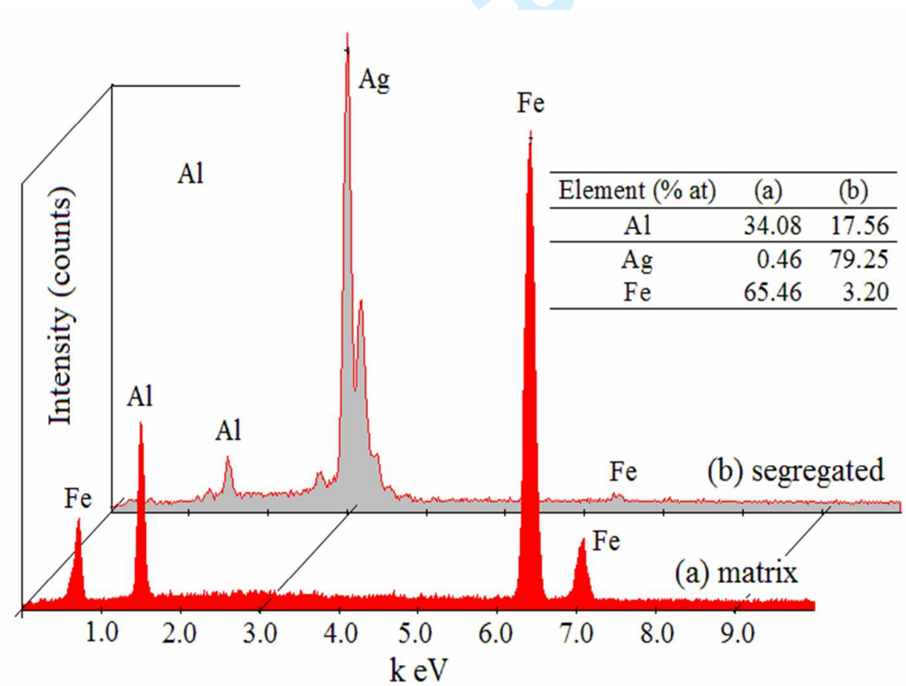
Ag
Fe
Al
Al
Al
Fe
Fe
Fe
Intensity (counts)
Element (% at) (a) (b)
Al 34.08 17.56
Ag 0.46 79.25
Fe 65.46 3.20
(b) segregated
(a) matrix
1.0 2.0 3.0 4.0 5.0 6.0 7.0 8.0 9.0
k eV

**Fig.5**

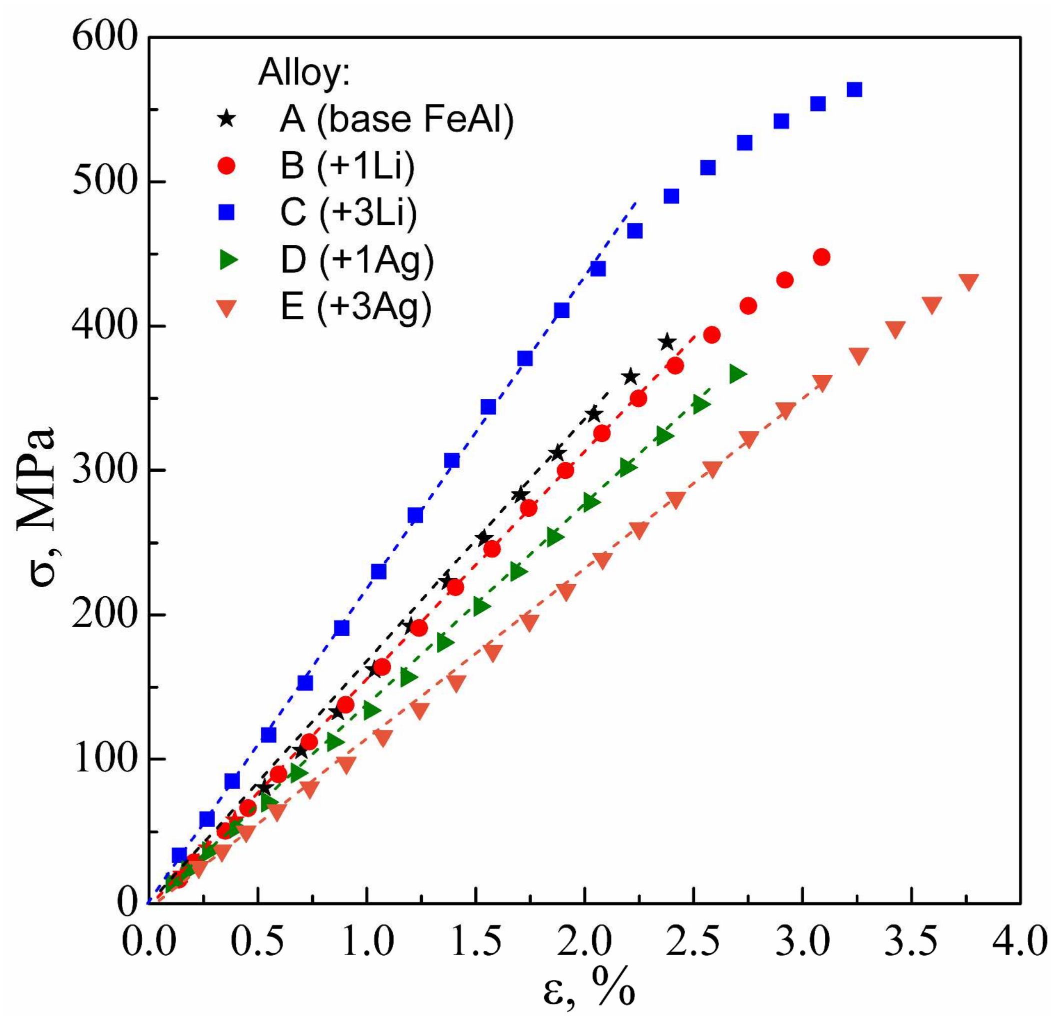
Alloy:
A (base FeAl)
B (+1Li)
C (+3Li)
D (+1Ag)
E (+3Ag)
σ, MPa
ε, %
0
100
200
300
400
500
600
0.0
0.5
1.0
1.5
2.0
2.5
3.0
3.5
4.0

**Fig.6**

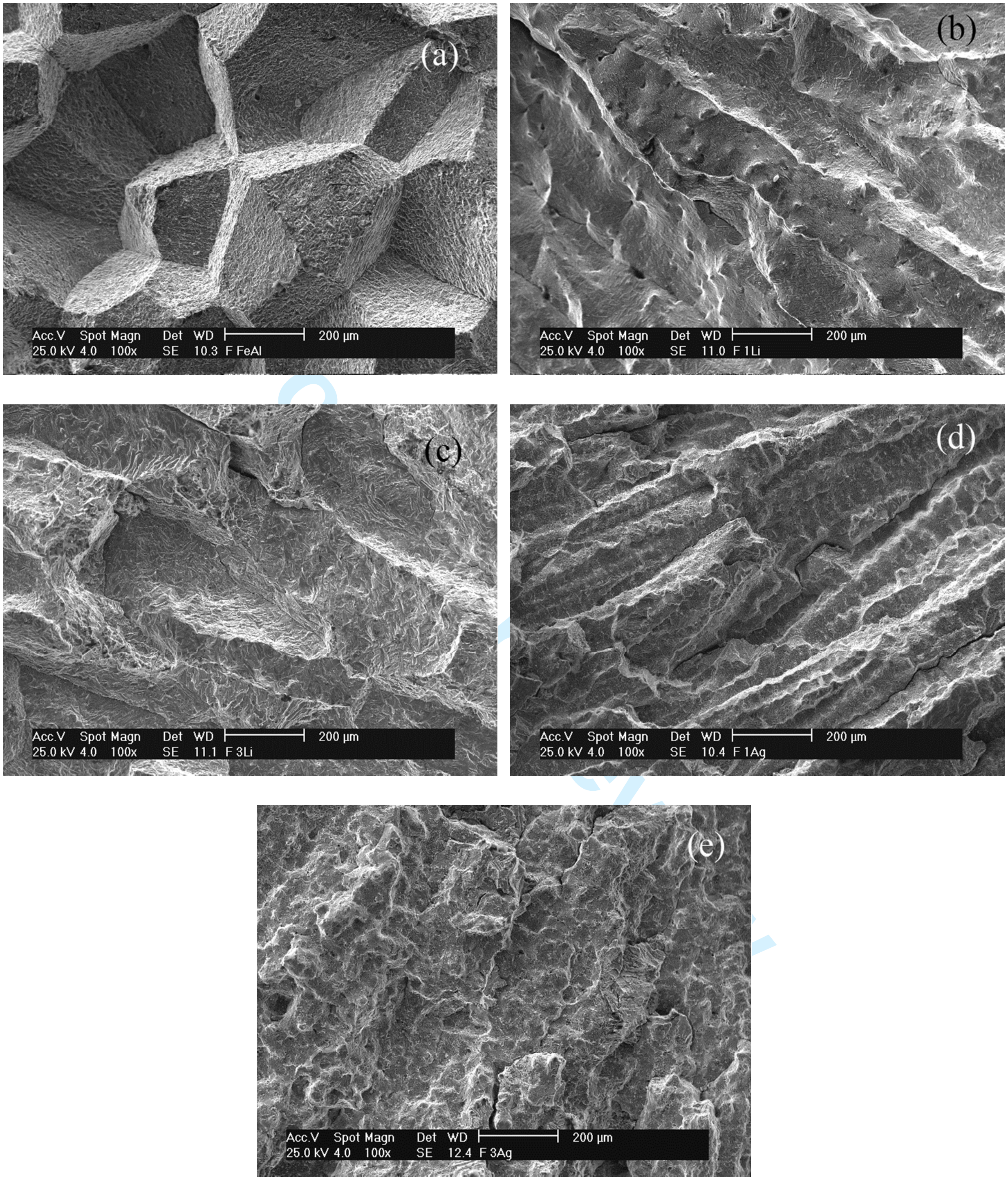
(a)
Acc.V Spot Magn Det WD 200 µm
25.0 kV 4.0 100x SE 10.3 F FeAl
(b)
Acc.V Spot Magn Det WD 200 µm
25.0 kV 4.0 100x SE 11.0 F 1Li
(c)
Acc.V Spot Magn Det WD 200 µm
25.0 kV 4.0 100x SE 11.1 F 3Li
(d)
Acc.V Spot Magn Det WD 200 µm
25.0 kV 4.0 100x SE 10.4 F 1Ag
(e)
Acc.V Spot Magn Det WD 200 µm
25.0 kV 4.0 100x SE 12.4 F 3Ag